Photocurable coatings with self-initiating and self-healing properties via dynamic disulfide bonds

Polymer 358 (2026) 130200

Contents lists available at ScienceDirect

Polymer

journal homepage: www.elsevier.com/locate/polymer

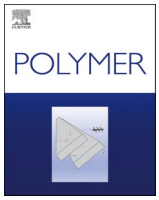

Photocurable coatings with self-initiating and self-healing properties via dynamic disulfide bonds⋆

Alberto Spessa [a,*], Franca Castiglione [d], Alice Rosanna Maggioni [a,b], Roberta Bongiovanni [a,c], Sara Dalle Vacche [a,c,**], Alessandra Vitale [a,c]

[a] Department of Applied Science and Technology, Politecnico di Torino, Corso Duca degli Abruzzi 24, 10129, Torino, Italy
[b] University School for Advanced Studies IUSS Pavia, 27100, Pavia, Italy
[c] INSTM – Politecnico di Torino Research Unit, 50121, Firenze, Italy
[d] Department of Chemistry, Materials and Chemical Engineering "Giulio Natta", Politecnico di Milano, Via Luigi Mancinelli 7, 20131, Milano, Italy

ARTICLE INFO

Keywords:
Photopolymerization
UV-Curable coatings
Dynamic covalent chemistry
Photoinitiator-free curing
Self-healing coatings

ABSTRACT

In the field of photocurable coatings, disulfide-containing monomers are gaining importance due to the unique properties and responsiveness of S–S bonds, which make them suitable for various applications, including photoinitiator-free and self-healable materials. In this work, a photocurable disulfide-containing polyurethane diacrylated monomer (DS-IPDA) was synthesized through a simple two-step addition reaction. First, the initiating ability of thiyl radicals, which are photogenerated by cleavage of disulfides by irradiation at wavelengths around 250 nm, was demonstrated by investigating the photopolymerization kinetics of the monomer in the presence or absence of a photoinitiator by FTIR analysis. Secondly, the dynamic nature of disulfide bonds and hence the self-healing ability of the coatings was assessed. Clear coatings were obtained by photocuring DS-IPDA alone or together with polyethylene glycol diacrylate at various weight ratios under a broadband (200 – 600 nm) ultraviolet (UV) light or under a UV LED light at 365 nm. The latter is safer and more energy efficient than traditional UV sources and helps preserve a higher content of unreacted disulfide bonds in the cured coatings for further use in dynamic covalent reactions. However, it requires the presence of a photoinitiator in the photocurable formulation. The disulfide exchange reaction proved effective in repairing surface damages after quick heat treatment. The incorporation of disulfide bonds imparting self-initiating or self-healing properties to coatings thus may contribute to improved sustainability reducing the number of components in the formulation by avoiding the use of potentially migrating photoinitiators and by extending product lifetime.

1. Introduction

Photopolymerization has inherently environmentally friendly and sustainable features, which have led to its growing significance and establishment as a reliable process in a wide range of fields [1–4]. Thanks to the low-energy demand, fast and controlled curing process, and absence of solvents, UV-curable materials are one of the main choices in several applications, primarily coatings, as well as 3D printing, biomedical materials, and optoelectronic components [5–8]. Despite its environmentally friendly features, photopolymerization still presents some drawbacks for its sustainability. Particularly, for UV-curable coatings the use of photoinitiators and the thermosetting nature of the photocured material are important issues [3,9–11].

Photoinduced polymerization relies on the propagation of a reactive radical, with varying chain length, generated through photocleavage of a specific photoinitiator [12]. Nevertheless, the presence of residual unreacted photoinitiator molecules or photodegradation products in the final cured coating can be deleterious for certain applications where the presence of small migrating species can be problematic, e.g., food packaging [13,14]. Moreover, more stringent regulations are arising concerning the potential effects on health of certain commercially available photoinitiators, thus limiting their use in UV-curable formulations [15]. In this scenario, reducing or avoiding photoinitiators in UV-curable formulations brings several advantages. Photoinitiator-free

⋆ This article is part of a special issue entitled: Polymer Coatings published in Polymer.

* Corresponding author.
** Corresponding author. Department of Applied Science and Technology, Politecnico di Torino, Corso Duca degli Abruzzi 24, 10129, Torino, Italy.
E-mail addresses: alberto.spessa@polito.it (A. Spessa), sara.dallevacche@polito.it (S. Dalle Vacche).

https://doi.org/10.1016/j.polymer.2026.130200
Received 20 February 2026; Received in revised form 23 April 2026; Accepted 10 May 2026
Available online 12 May 2026

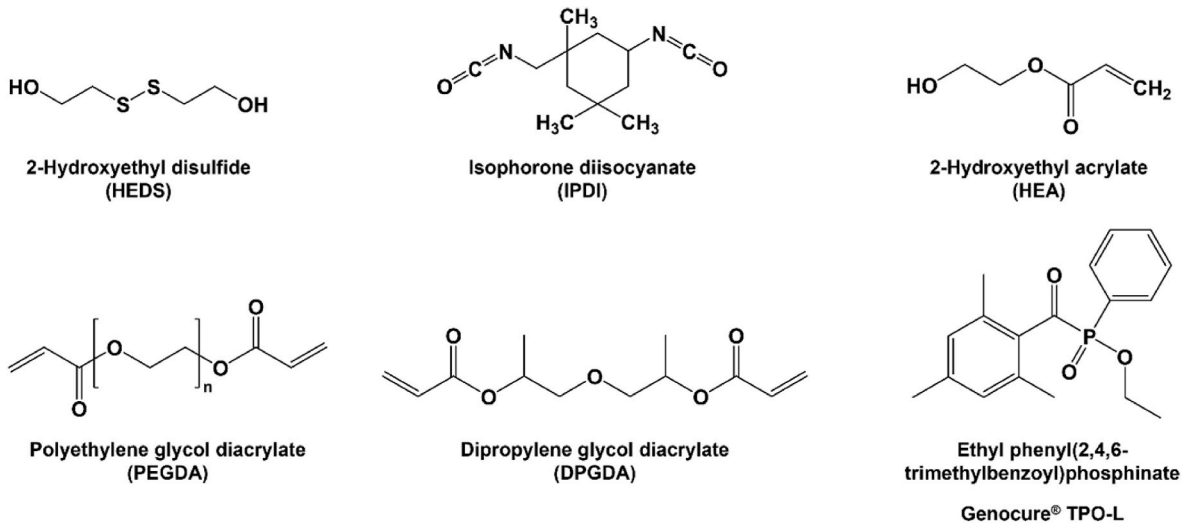

Fig. 1. Structures of chemicals used.

formulations can be designed by incorporating specific monomers, such as diacrylamides, or systems such as thiol-ene or bismaleimides [16–21]. More recently, disulfide bonds and related chemistry have been used as an initiating mechanism for acrylic formulations [22–25]. When exposed to UV light, disulfides are promptly cleaved, generating reactive thiyl radicals, which are able to start the polymerization reaction [23, 25–27].

The thermosetting nature of photocured resins offers several advantages in terms of mechanical and chemical resistance of the materials; however, it also limits their potential for reuse, reprocessing or recycling once crosslinked, arising environmental concerns [28–30]. To overcome this issue, dynamic covalent bonds have been explored as a possible solution to increase the recyclability of the photocured networks, introducing the capability to change the network structure in response to external stimuli [11,31–35]. In the coatings industry, providing a healing solution for surface damage is also of primary importance. Coatings are susceptible to scratching during use, which has a detrimental effect on both their lifespan and intrinsic value [36,37]. In this scenario, the implementation of UV-curable coating bearing dynamic functionalities, allowing damage healing, has gained importance [38].

Among different types of dynamic covalent bonds, disulfides are very attractive due to their responsiveness to several external stimuli such as temperature, light, pH, and reductive agents [39–42]. Either used alone or coupled with reactive thiol groups, disulfide bonds may undergo a series of exchange reactions, such as disulfide metathesis or thiol-disulfide exchange [43,44]. These on-demand molecular rearrangements can be exploited to repair mechanical damage or reprocess the material once crosslinked [42,45,46].

Different studies have reported the use of disulfide-containing compounds in photo- or thermally curable formulations, to achieve self-repairing and self-healing properties by applying light [47] or heat [48], relying on disulfide exchange reactions. The incorporation of bis (2-methacryloyl)oxyethyl disulfide in a classical bisphenol A diglycidyl ether dimethacrylate UV-curable formulation allowed the successful thermally-induced healing of the photocured coating [41]. Disulfide-containing diamines with different proportions of flexible segments were used to cure a polyurethane-modified epoxy resin, showing that the efficiency of the thermally induced healing was influenced by the content of dynamic bonds and by chain flexibility [49].

Monomers and prepolymers containing both disulfide and urethane functional groups have been synthesized for different applications. Self-healing ability was imparted to spray paint or cast and thermally crosslinked polyurethane coatings [50,51] and poly(urethane-urea) coatings [52]. A self-healing polyurethane elastomer [53] and a self-repairable, recyclable, and shape memory castor oil-based polyurethane acrylate [54] suitable for Digital Light Processing (DLP) 3D printing applications, were reported. In addition, a polyurethane acrylate prepolymer containing a disulfide bond and a flexible polycaprolactone-diol chain was synthesized and used as a debondable UV-curable adhesive, exploiting the reversibility of the disulfide bond within crosslinked networks [55]. More specifically, different disulfide-containing polyurethane acrylates have been employed either as neat resins or in combination with conventional photocurable acrylic resins to obtain coatings with self-healing ability [40].

Previously [56], we reported a disulfide-containing polyurethane diacrylate monomer exhibiting both UV-induced self-initiation and thermally activated self-healing. However, its solid-state nature at room temperature limited processability and practical use in coating formulations. To overcome this limitation, we synthesized a structurally related monomer inspired by Zhang et al. [57], featuring improved handling characteristics. Beyond formulation aspects, this study provides a systematic investigation of its photopolymerization behaviour and network structure. Real-time curing kinetics were analysed, and self-initiation and self-healing were evaluated for both homopolymer networks and copolymers prepared with a conventional diacrylate. This approach clarifies the relationship between disulfide content, network mobility, and healing efficiency in photocurable polyurethane acrylate systems.

2. Materials and methods

2.1. Materials

2-Hydroxyethyl disulfide (HEDS), isophorone diisocyanate (IPDI), 2-hydroxyethyl acrylate (HEA), poly(ethylene glycol) diacrylate (PEGDA) with average M_n of 575, 2,6-di-*tert*-butyl-4-methylphenol (BHT), and dibutyltin dilaurate (DBTL) were purchased from Sigma Aldrich. Dipropylene glycol diacrylate (DPGDA), used as a reactive diluent, and ethyl phenyl(2,4,6-trimethylbenzoyl)phosphinate (Genocure® TPO-L), used as a photoinitiator for the polymerization reaction were kindly provided by Rahn AG, Switzerland. The chemical structures of the reagents are summarized in Fig. 1.

All other solvents used were purchased from Sigma-Aldrich. All the reagents were used without any further purification.

Table 1
Labels and compositions of the prepared formulations.

Formulation	DS-IPDA [wt%]	PEGDA [wt%]	Genocure® TPO-L [phr]
DS-IPDA	100	0	0
DS-IPDA 100	100	0	1
DS-IPDA 75	75	25	1
DS-IPDA 50	50	50	1
PEGDA	0	100	1

2.2. Synthesis of DS-IPDA

A disulfide-containing polyurethane diacrylate (DS-IPDA) monomer with the molecular structure proposed by Ref. [57] was synthesized according to a well-established two-step addition reaction scheme commonly used for polyurethane synthesis [53,58,59].

In the first step IPDI (159.92 g, 0.72 mol), BHT, and DBTL were added to a round-bottom reaction flask. The mixture was first stirred and then HEDS (55.81 g, 0.36 mol) was added dropwise to the reaction mixture through a graduated dropping funnel. The mixture was stirred for 2 h before proceeding with the following step. As already reported for the synthesis of another disulfide-containing urethane monomer [56], the exothermic reaction given by the urethane bond formation between hydroxyl groups of HEDS and isocyanate moieties of IPDI was constantly monitored and kept in the range of 50-60 °C using a cold bath.

In the second step, HEA (84.01 g, 0.72 mol) was added dropwise to the reactor, using a graduated dropping funnel. As performed for the first step, the exotherm given by urethane bond formation between the step-one product and the HEA was kept below 60 °C, to avoid overheating of the reaction. Due to the high viscosity developed in the reaction flask, a difunctional reactive diluent, DPGDA (75 g, 20 wt%), was added to the mixture as a diluent. To simplify the notation, the mixture of DS-IPDA and DPGDA will be referred to just as DS-IPDA in the following sections. The presence of unreacted isocyanate was assessed through FTIR analyses, checking the disappearance of the –NCO stretching peak around 2260 cm^{-1}. The reaction proceeded until the remaining amount of isocyanate groups was lower than 0.3% (~20 h). A steady air inlet was constantly fluxed into the reaction flask to inhibit the polymerization of the reacting mixture.

2.3. DS-IPDA coatings preparation

Coating formulations were prepared using DS-IPDA alone or by mixing it with PEGDA using different ratios, up to 50:50 w/w, as well as PEGDA alone used as reference; 1 part per hundred resin (phr) of Genocure® TPO-L was then added to each formulation, except the self-initiating DS-IPDA one, mixing for 15 min to ensure complete dispersion of the photoinitiator. The compositions of the different formulations tested are reported in Table 1.

Each formulation was spread on a glass slide with a 50 μm wire-wound applicator to obtain a homogeneous layer of material. Given the high viscosity of the synthesized DS-IPDA, the formulations that did not contain PEGDA (i.e. DS-IPDA and DS-IPDA 100) were heated to 50 °C in an oven before spreading on glass slides, thus facilitating the coating procedure. Coatings with photoinitiator were then cured using a UV LED spot curing system operating at 365 nm (OmniCure® LX500, Excelitas) with an intensity of 100 mW cm^{-2}. The UV LED light intensity was quantified using a UV Power Puck® II (EIT® Instrument Markets). The coating samples were irradiated for 120 s under an inert atmosphere to allow complete curing of the samples. The self-initiating DS-IPDA coating was cured using a mercury-xenon lamp (LIGHTNINGCURE™ Spotlight source LC8, Hamamatsu) having a spectral distribution in the 200 – 600 nm range, using the same conditions of time and intensity as for the LED cured coatings. In this case the light intensity was evaluated using a UV Handheld Meter HI1 (UV-Technik international LTD) equipped with the sensor SI1 UV Gesamt 230-410 nm 200 $mWcm^{-2}$. The final thickness of the coatings was in the 75 – 85 μm range.

For self-healing and hardness measurements, self-standing films in the form of disks with a diameter of 12 mm and a thickness around 770 μm were prepared using a silicon mould. The curing was performed with the same procedures as for the coatings; only in the case of DS-IPDA it was necessary to increase the irradiation time, 10 min on each side, to obtain solid films.

2.4. Characterization

The molecular weight distribution of the synthesized DS-IPDA was investigated by gel permeation chromatography (GPC) using an Ercatech GPC system. Tetrahydrofuran (THF) was used as the eluent for the samples, imposing an injection volume of 100 μL and a mobile phase flow rate of 1.0 mL min^{-1}.

NMR spectroscopy was used to investigate the chemical structure of the product after synthesis. 1D and 2D NMR experiments were performed on a Bruker NEO console operating at 400 MHz. The sample was dissolved in chloroform (10 mg mL^{-1}) which was used as an internal deuterium lock. Chemical shifts (δ) are reported in parts per million (ppm) using the residual $CDCl_3$ as a reference. The experimental conditions are: ^{1}H spectrum (16 scans and 10 ppm sweep width); ^{13}C-$^{1}\{H\}$ and ^{13}C-$^{1}\{H\}$ DEPT experiments (2048 scans, 200 ppm sweep width and D1 of 5 s). 2D ^{1}H–^{1}H COSY spectrum was recorded with a spectral width of 10 ppm, 4 scans, 512 increments in t1, and 2048 complex data points in t2. Natural abundance heteronuclear ^{13}C-{^{1}H} HSQC spectrum was acquired with 512 t1 increments and 1024 complex data points in t2, using a sweep width of 10 ppm in the proton and 200 ppm in the carbon dimension.

The photocleavage of DS-IPDA upon UV light irradiation with different wavelengths was investigated using a Thermo Fisher Scientific Evolution 220 UV-Vis spectrophotometer in absorbance mode. For irradiation experiments, DS-IPDA was dissolved in a suitable amount of anhydrous methanol and placed into a 10 mm quartz cuvette. UV-Vis spectra were acquired before and after UV exposure at different times. Irradiation of the DS-IPDA/methanol solution was performed with the two light sources used for photocuring: the UV LED spot curing system operating at 365 nm (OmniCure® LX500, Excelitas), and the mercury-xenon lamp (LIGHTNINGCURE™ Spotlight source LC8, Hamamatsu). In both cases, the intensity of the UV light was set to 100 mW cm^{-2}.

The conversion of acrylate groups was evaluated at discrete time intervals during photocuring by FTIR spectroscopy analyses by using a Thermo Fisher Scientific Nicolet™ iS50 spectrometer in transmission mode in the spectral range of 4000–400 cm^{-1}. 10 μm-thick films were cast on a silicon wafer and irradiated for up to 350 s in an inert atmosphere (N_2), and spectra were collected at fixed time intervals with 32 scans per spectrum and a resolution of 4 cm^{-1}. The value of acrylate conversion was calculated according to Eq. (1).

$$Conversion\% = \left(1 - \frac{A_t}{A_0}\right) \times 100 \qquad \text{(Eq. 1.)}$$

where A_t is the normalized area of the peak of the reactive group (acrylate C═C double bond at 1635 cm^{-1}) at time t of irradiation and A_0 is the normalized area of the same peak before irradiation. The area of the C═O stretch peak centered at 1720 cm^{-1} was used as an internal reference for normalization.

Photopolymerization kinetics of LED cured formulations were investigated using real-time FTIR (rt-FTIR) spectroscopy in transmission mode using the same Thermo Fisher Scientific Nicolet™ iS50 spectrometer fitted with a custom accessory for *in situ* irradiation, working in the spectral range of 2700-400 cm^{-1}. DS-IPDA/PEGDA films were prepared by spreading the formulation on a silicon wafer using a 10 μm manual wire-wound applicator. Samples were then irradiated for 120 s using the same LED spot curing lamp (OmniCure® LX500, Excelitas)

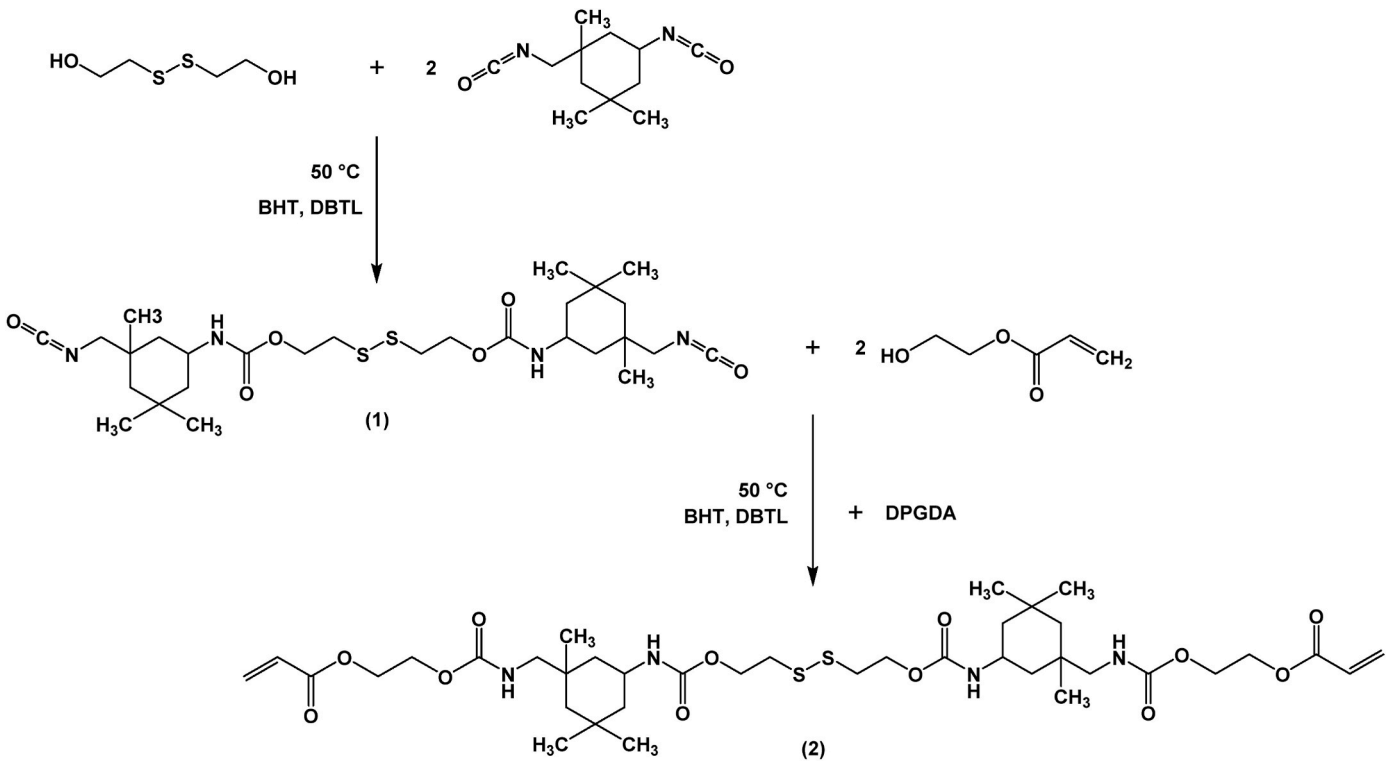

Fig. 2. Synthesis reaction of DS-IPDA.

previously employed, placing the optical fibre at a distance of 5 cm from the surface of the sample. The light intensity was set at 100 mW cm^{-2}. The intensity of incident light was assessed by means of UV Power Puck® II (EIT® Instrument Markets). In order to carry out the polymerization under inert conditions and thus avoid oxygen presence on the sample surface, formulations were covered with a 50 μm polyethylene film during measurements, aiming to hinder the oxygen inhibition on the surface of the samples. FTIR spectra were recorded continuously during irradiation, setting the sampling rate at 50 spectra per minute. For each measure, the UV lamp was switched on 30 s after the beginning of data acquisition. The acrylate group conversion was calculated according to Eq. (1) as a function of time. Starting from the kinetic curve (double bond conversion vs time of irradiation), the photopolymerization rate was calculated as the first-order derivative of the curve. Three different kinetic curves were registered for each sample and then averaged to calculate the final conversion value. The standard deviation for each conversion kinetics was in the range between 1 and 5%.

The gel fraction, and thus the amount of insoluble photocured coating, was assessed by gel content analysis, evaluating the weight difference for each sample after 24 h of extraction in acetone at room temperature. After being immersed in the solvent, the samples were left to dry first under the fume hood for 24 h, then in the oven at 60 °C for 5 h and 80 °C for two more hours.

The viscosity (η) of DS-IPDA/PEGDA formulations was measured respectively at 25 °C and 50 °C by using an Anton Paar MCR 702e MultiDrive Rheometer (Graz, Austria) in a parallel plate configuration. The measures were conducted in a shear rate range of 0.1-100 s^{-1}, assessing the value of viscosity from the plateau region of the curve.

Thermal properties of the synthesized DS-IPDA were examined by differential scanning calorimetry (DSC), conducted with a Mettler Toledo DSC 3+, placing a total amount of 13.5 mg into a sealed aluminum pan. The uncured DS-IPDA monomer was subjected to heating/cooling cycles ranging from −70 °C to 100 °C with a heating/cooling rate of 10 °C min^{-1}. All DSC analyses were performed under N_2 flux (50 ml min^{-1}). The thermal properties of photocured DS-IPDA/PEGDA samples were measured using a Q20 TA Instrument by placing samples of about 5 mg in sealed aluminum pans. All the experiments performed were conducted under N_2 flux (50 ml min^{-1}). Samples were subjected to heating/cooling cycles ranging from −70 °C to 180 °C with a heating/cooling rate of 10 °C min^{-1}. In all cases, the midpoint of the inflection was employed to estimate the glass transition temperature (T_g).

The UV-Vis transmittance was evaluated on 50 μm cured DS-IPDA/PEGDA coatings using a Thermo Scientific™ Evolution™ One series UV-Visible spectrophotometer. The spectra were collected in transmittance mode in the range of 300-1000 nm with a bandwidth of 1 nm.

The wettability properties of photocured DS-IPDA/PEGDA coatings were determined using static contact angle analyses by means of an FTA 1000C instrument (First Ten Angstroms) equipped with a video camera and image analyzer software. Five measurements were obtained for each coating sample, and the mean value and associated error were subsequently calculated. Two probe liquids with different surface tensions were employed: water (surface tension = 72.1 mN m^{-1}) and hexadecane (surface tension = 28.1 mN m^{-1}). The surface energy of the sample analysed was then calculated according to the Owens-Wendt geometric mean method [60].

The surface hardness of cured DS-IPDA/PEGDA formulations was assessed through a shore D durometer hardness apparatus (SAUTER HBD 100-0 by Sauter GmbH). The samples analysed were in the form of disks with a diameter of 12 mm and a thickness of around 770 μm (prepared as explained above), and they were tested at room temperature.

The adhesion level of the various coatings was evaluated following the method of the standard ISO 16276-2:2007 on a glass substrate, using a TQC sheen kit. A X-cut was performed with a single blade cutter, and then a transparent pressure-sensitive tape was applied on top and then removed at 180°. The adhesion was estimated by inspecting the undamaged coating after tape removal and scored following the scale given by the standard, going from 0 in case of no peeling or removal up to 5 for a removal beyond the area of the X-cut.

The resistance of the DS-IPDA/PEGDA coatings to solvent was

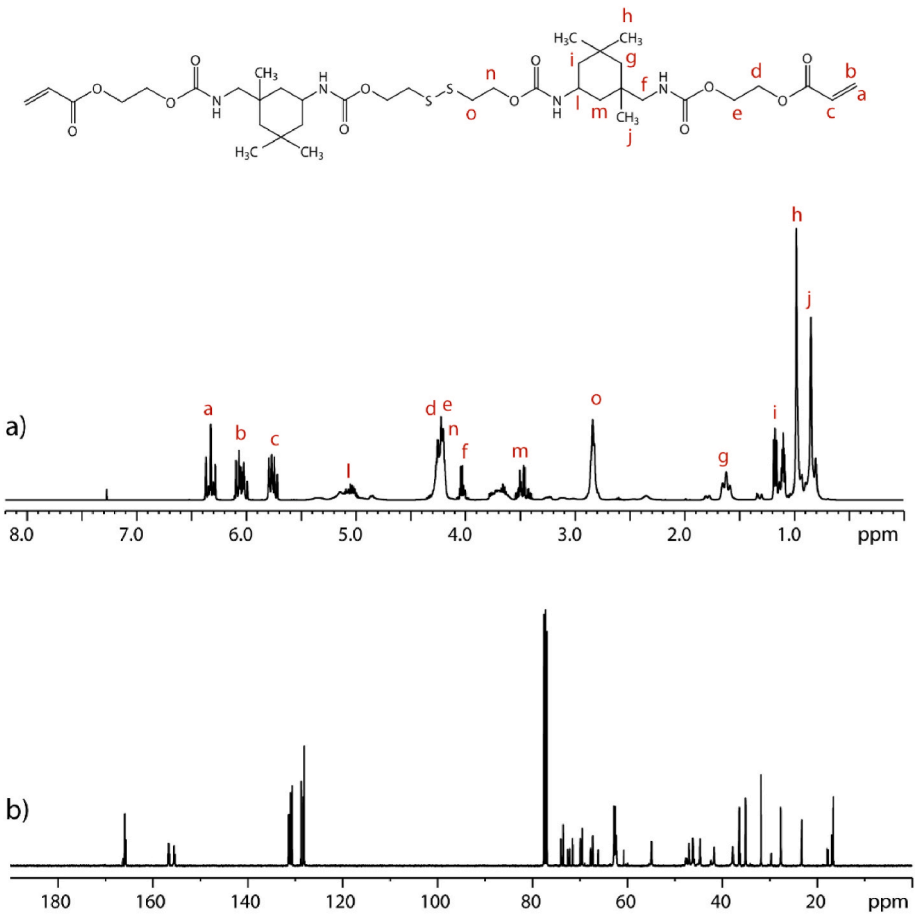

Fig. 3. (a) ^{1}H NMR and (b) ^{13}C NMR spectra of DS-IPDA after synthesis reaction.

investigated using an adapted version of ASTM D5402 [61]. The surface of the coating was rubbed with an ethyl acetate-soaked cloth, and coating solvent resistance was identified as the number of double rubs required to create a damage or a scratch on the surface of the sample.

The self-healing ability of the obtained networks was assessed by testing the healing of surface scratches or cuts following a heat treatment. Surface scratches were obtained on coatings with a sharp metal tip (obtaining 7 – 25 μm wide scratches, depending on the coating type) and with a surgical blade, obtaining thin surface scratches. Without applying any external force, the damaged samples were heat-treated in a convection oven with temperatures ranging from 55 °C to 130 °C. Also, cuts obtained with a surgical blade on DS-IPDA 75 and DS-IPDA 50 self-standing films were healed in a heated press (Mini-Film Maker Kit GS03970, Specac) for 15 min applying a force of 0.5 – 0.7 ton, at temperatures of 85 °C and 55 °C, respectively. Optical microscope images were taken before and after the thermal treatment, using an Olympus BX53MRF-S optical microscope equipped with a digital camera, with a magnification of 20×. A visual qualitative assessment was done for the healing of thin surface scratches, while the healing of larger surface scratches and cuts was quantitatively assessed by measuring the reduction of the width of the damaged area (image analysis was performed using Adobe Photoshop software, Adobe Inc.).

3. Results and discussion

3.1. Synthesis of DS-IPDA

A disulfide-containing polyurethane diacrylate monomer (DS-IPDA) was synthesized through a two-step addition reaction between a hydroxyl-terminated disulfide (HEDS), IPDI, and HEA [59]. A general scheme of the reaction is depicted in Fig. 2. In the first step, HEDS was reacted with IPDI, at 50 °C in the presence of a catalyst, yielding an isocyanate end-capped disulfide intermediate (1). Product (1) then underwent a second addition reaction with HEA to introduce the terminating acrylic groups on the isocyanate groups and to obtain the final product (2). To decrease the viscosity of the medium and enhance its suitability for industrial applications, 20 wt% of a low-viscosity difunctional reactive diluent (DPGDA, $\eta = 15$ mPa s^{-1}) was added.

The synthesis of DS-IPDA was monitored by GPC and NMR. The obtained GPC chromatogram is reported in Fig. S1. Several peaks were present: the small peak at 18.6 min could be assigned to the unreacted HEA still present in the mixture, while the two following peaks, respectively at 17.8 and 17.2 min, were attributed to DPGDA added as a viscosity modifier. The high peak at 16.5 min was reasonably due to the formation of a diacrylate monomer between unreacted IPDI and HEA since no purification step was done between the two addition reactions during the synthesis procedure. The highest peak at 15.5 min was related to the final product (2), thus DS-IPDA. Multiple peaks between 14.8 min and 13 min were attributed to high-molecular-weight byproducts, given by the uncontrolled addition of IPDI on HEDS during the first addition reaction. This undoubtedly led to the formation of a series of oligomers formed by the subsequent repetition of HEDS-IPDI units, which were acrylated during the second addition reaction with HEA. Since the stoichiometric reaction in which one molecule of HEDS reacts with two molecules of IPDI was no longer valid, an excess of IPDI was present in the reaction mixture. The formation of diacrylated IPDI served as further evidence in support of this hypothesis.

^{1}H and ^{13}C-{^{1}H} NMR spectra of DS-IPDA polymeric mixture, obtained after reaction, are shown in Fig. 3 (a and b respectively). The proton spectrum was assigned using the 2D ^{1}H–^{1}H COSY, ^{13}C-{^{1}H}

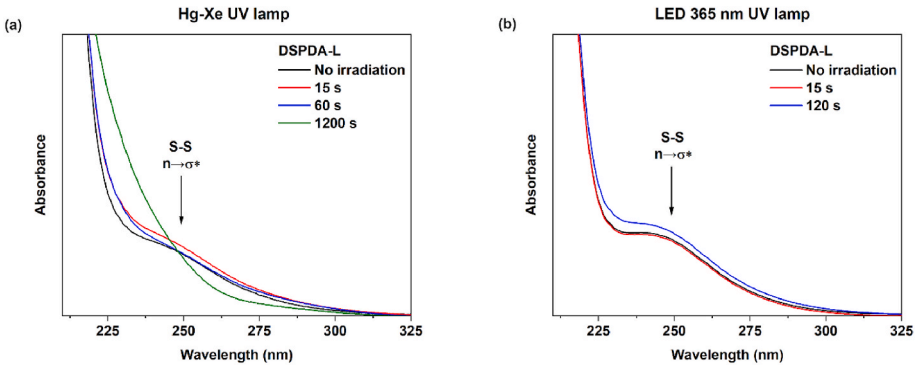

Fig. 4. UV-Vis photolysis spectra of DS-IPDA solution in methanol when exposed to (a) a mercury-xenon UV lamp and to (b) a UV LED lamp operating at 365 nm.

HSQC and ^{13}C-{^{1}H} DEPT experiments (Fig. S2–S4) and are in agreement with literature data [57]. A careful observation of the NMR spectra, both proton and carbon, shows multiple signals, most visible in the 5.5-6.5 ppm region, thus indicating the presence of high-molecular-weight polymers or unreacted species, as also seen by GPC. Chemical shifts and integrals of relevant proton signals are reported in Table S1.

Given that all the molecules present in the mixture obtained after the reaction contained a reactive acrylate group, thereby enabling their participation in the polymeric network formation upon irradiation, in addition to one or more disulfide dynamic bonds, it was considered unnecessary to purify the obtained mixture, in view of a simpler scale-up of the process. The mixture under discussion has been designated DS-IPDA in the ensuing sections to facilitate the notation.

DSC was used to investigate the thermal transitions of the synthesized DS-IPDA: the obtained curve is reported in Fig. S5. The glass transition temperature was assessed at approximately −9.7 °C, while no melting or crystallization temperatures were present in the curve within the tested temperature range (−70 °C – 100 °C). At room temperature, the monomer mixture is in fact a highly viscous liquid (non-crystalline), owing its amorphous structure to the presence of the IPDI building block. This, in fact, has a high steric hindrance limiting the formation of hydrogen bonds between urethane groups, and an asymmetric structure with *cis*- (Z) and *trans*- (E) isomers that does not favour the formation of a crystalline phase [50,62].

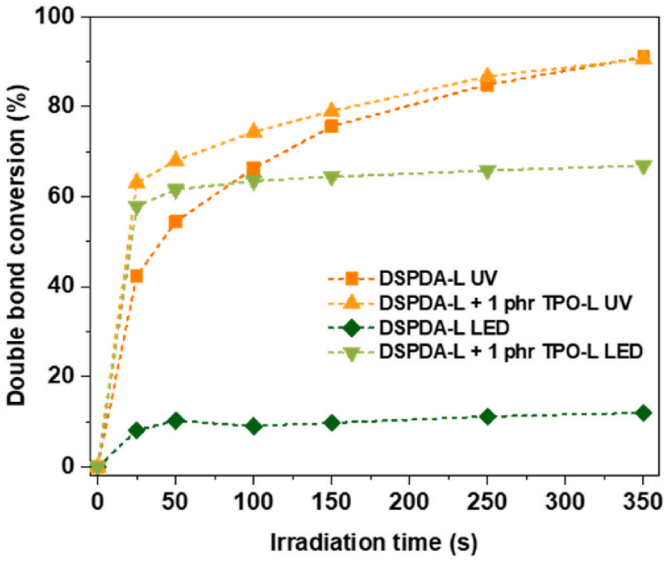

Fig. 5. Double bond conversion of DS-IPDA cured with mercury-xenon UV lamp (100 mW cm^{-2} ■ without photoinitiator, and ▲ with photoinitiator) and DS-IPDA cured with UV LED lamp (100 mW cm^{-2} ◆ without photoinitiator, and ▼ with photoinitiator).

3.2. Photopolymerization of DS-IPDA

The initial step in the study of the photopolymerization of the synthesized DS-IPDA was the investigation of UV-induced disulfide bond photocleavage, to demonstrate the self-initiation ability of the system. As demonstrated in previous studies [26,63,64], disulfide bonds are susceptible to UV light, resulting in photocleavage and the subsequent production of thiyl radicals. These thiyl radicals are able of reacting in different chemical processes [23,27], including the initiation of polymerization [24,56].

First, methanol solutions of DS-IPDA were prepared and analysed with UV-Vis spectroscopy. As shown by the absorption spectra of DS-IPDA (Fig. 4), an absorption peak appeared around 249 nm, ascribable to the n→σ* electronic transition of the disulfide bond. DS-IPDA methanol solutions were then irradiated under UV light using two different types of light sources with different emission ranges: a mercury-xenon UV lamp (emission range 200 nm - 600 nm) and a UV LED lamp (emission range 360 nm – 370 nm). UV-Vis absorption spectra of DS-IPDA in methanol solution before and after UV light exposure for both UV lamps are reported in Fig. 4.

When the DS-IPDA solution was exposed to UV light from a mercury-xenon lamp, the intensity of the peak related to the n→σ* electronic transition of the S–S bond decreased, as previously reported for HEDS [56]. The peak completely disappeared after 1200 s of irradiation. In contrast, when the same DS-IPDA methanol solution was irradiated using a UV LED lamp operating at 365 nm, the absorption peak of the S–S bonds centered around 249 nm did not decrease and remained constant with increasing time of irradiation. As expected, wavelengths in the UV-C region (UV light with wavelengths below 280 nm) can promote disulfide cleavage.

To further assess DS-IPDA self-initiating ability, FTIR spectroscopy was used to quantify the acrylate double bonds conversion in the absence or presence of a Norrish type I photoinitiator (i.e., TPO-L). Samples were irradiated with either a mercury-xenon UV lamp or a UV LED lamp to benchmark the initiation ability of DS-IPDA when different light sources were employed. As illustrated in Fig. 5, the DS-IPDA system exhibited similar levels of double bond conversions (90%) in the presence and absence of a photoinitiator when photocured with a mercury-xenon UV lamp curing system. In this instance, the initiating effect of thiyl radicals obtained by photocleavage of disulfide bonds present in DS-IPDA was confirmed, despite the initial polymerization rate being slower in comparison to that achieved in the presence of TPO-L.

When the same photocuring process was performed using a UV LED lamp emitting 365 nm light, a considerable level of double bond conversion was only achieved in the presence of a photoinitiator. This resulted in approximately 67% conversion after 350 s of irradiation. In

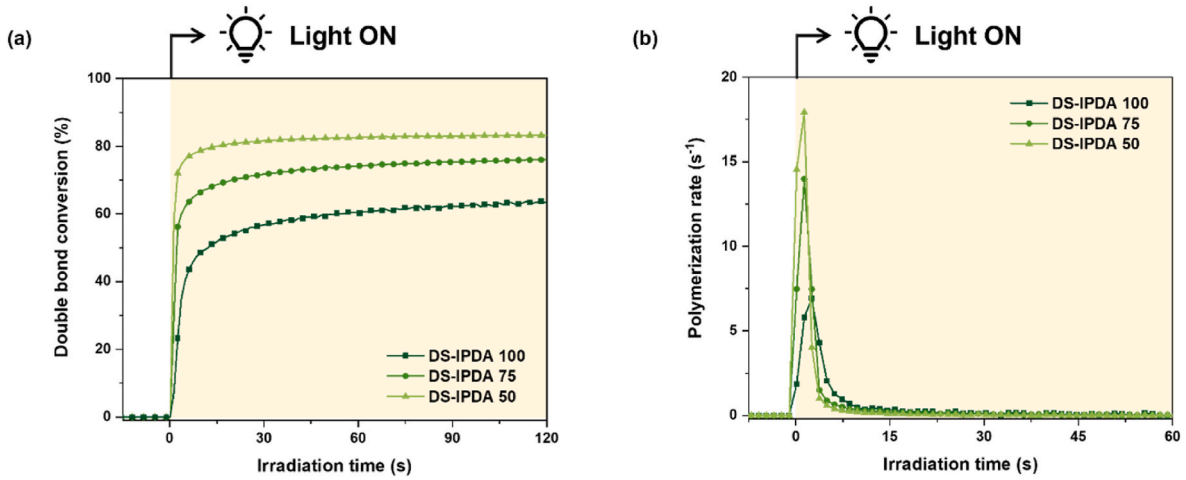

Fig. 6. Photocuring kinetics curves of DS-IPDA/PEGDA samples. (a) Conversion of acrylate double bonds over irradiation time and (b) polymerization rate over irradiation time.

Table 2
Double bond conversions and polymerization rate values of materials cured by LED light at 365 nm with 1 phr photoinitiator.

Formulation	η (25 °C, 10 s^{-1}) [mPa s]	Double bond conversion [%]	Polymerization rate [s^{-1}]
DS-IPDA 100	5.83×10^5	66	7
DS-IPDA 75	1.09×10^4	76	14
DS-IPDA 50	8.05×10^2	83	18

contrast, the DS-IPDA sample without photoinitiator reached only 12 % of double bond conversion. This confirmed that UV LED irradiation at 365 nm is insufficient to induce disulfide homolysis and generate initiating thiyl radicals. This behaviour is consistent with the UV-Vis results, and therefore indicates that under these conditions, an external photoinitiator is required to effectively trigger polymerization. It is also worth noting that curing DS-IPDA with the mercury-xenon UV lamp led to a higher final conversion compared to LED irradiation, even in the presence of photoinitiator. This suggests differences in the polymerization pathway and network development. In the case of broadband irradiation, the continuous generation of thiyl radicals via disulfide cleavage may promote a more progressive network build-up, delaying vitrification and preserving molecular mobility to higher conversions. Conversely, LED-induced curing in the presence of a photoinitiator likely leads to a faster initial radical flux and earlier diffusion-controlled termination, limiting the attainable final conversion.

Due to the high viscosity of DS-IPDA, the resin was mixed with PEGDA in different amounts, namely 25 wt% and 50 wt%: as a reactive diluent, PEGDA limits the drawbacks viscosity poses to processing. The viscosity *vs* shear rate curves measured for the DS-IPDA/PEGDA formulations are reported in Fig. S6. The viscosity curves for DS-IPDA 100 formulation were collected at room temperature (i.e. 25 °C), and at 50 °C to simulate the coating preparation conditions. As expected, increasing the temperature significantly reduced the viscosity, facilitating film deposition. When PEGDA was added to the DS-IPDA, the viscosity value dropped by three orders of magnitude, shifting from 5.83×10^5 mPa s for DS-IPDA 100 to 8.05×10^2 mPa s for the formulation with 50% w/w PEGDA (DS-IPDA 50). In addition to efficiently reducing the viscosity of the formulations, PEGDA has a flexible structure that contributes to increasing chain mobility (an important parameter for dynamic bond exchange and self-healing), while its difunctional structure allows it to actively participate in the formation of the crosslinked network.

Curing kinetics under UV LED light at 365 nm was studied for coatings in the presence of 1 phr of TPO-L radical photoinitiator by real-time FTIR measurements. Conversion curves and polymerization rates over irradiation time are reported in Fig. 6, while double bond conversion values and polymerization rates for all the samples are summarized in Table 2.

By increasing the amount of PEGDA in the formulations, the final double bond conversion increased, reaching 83% in the case of DS-IPDA 50. The photopolymerization rate followed the same trend, with the highest rate of 18 s^{-1} for the sample containing the highest amount of PEGDA. Reasonably, the slower polymerization rates and the smaller double bond conversions in the presence of a higher amount of DS-IPDA were not due to a lack of reactivity of the disulfide-containing monomer, but to the high viscosity of DS-IPDA 100 (Table 2) and to the earlier onset of vitrification, both hindering reactive groups mobility during the

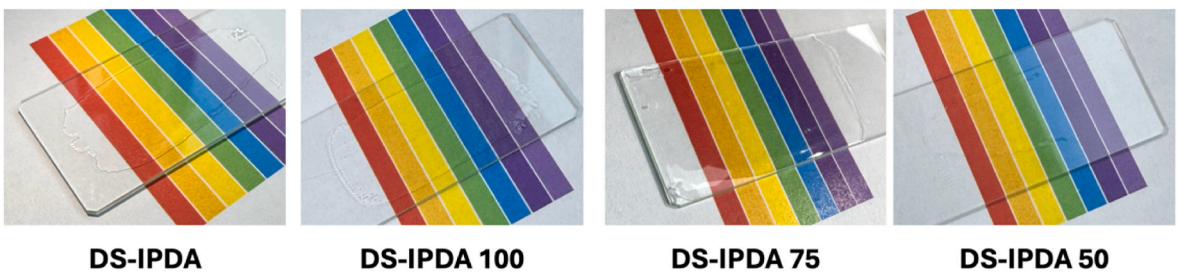

Fig. 7. Images of photocured DS-IPDA based coatings on glass slides.

Table 3
Gel fraction, glass transition temperature (T_g), contact angles of water and hexadecane with the respective surface energies and components, hardness and solvent resistance values for coatings cured for 2 min.

Samples	DS-IPDA	DS-IPDA 100	DS-IPDA 75	DS-IPDA 50
Gel fraction [%]	36	98	91	96
T_g [°C]	45.4	80.8	64.9	36.9
θ_w [°]	61.4 ± 0.5	72.6 ± 1.2	68.4 ± 2.3	64.0 ± 1.8
θ_h [°]	10.1 ± 0.6	13.8 ± 1.6	11 ± 0.2	8.6 ± 0.8
γ_S [mN m^{-1}]	44.2	37.2	39.8	42.6
γ_S^D [mN m^{-1}]	27.1	26.7	27	27.2
γ_S^P [mN m^{-1}]	17.1	10.5	12.8	15.4
Hardness [shore D]	N.A.	78 ± 2	77 ± 1	73 ± 3
Solvent resistance [# double rubs]	-	20	40	90

photoinduced polymerization reaction.

Thus, the addition of the PEGDA comonomer not only enables processing at room temperature by providing suitable viscosity for coating but also increases the conversion degree and accelerates the reaction imparting sufficient chain mobility during photocuring.

3.3. DS-IPDA based coatings characterization

Since the synthesized DS-IPDA could be easily and rapidly photocured alone or mixed with PEGDA to obtain a consistent transparent film (shown in Fig. 7), its application as a potential thin coating was studied and investigated. DS-IPDA based coatings cured for 120 s with a 365 nm UV LED lamp in the presence of TPO-L photoinitiator were prepared according to the formulations described in Table 1. This approach allows to maximize the amount of dynamic covalent bonds in the cured samples and provides a safer and more energy-efficient curing process compared to conventional UV sources, however, under these conditions, the use of a photoinitiator is required to achieve satisfactory conversion. Self-initiated coatings were obtained by curing the bare DS-IPDA for 120 s under the mercury-xenon UV lamp, exploiting the photopolymerization promoted by thiyl radicals.

All coatings were transparent and colourless. Their optical transmittance was evaluated by UV–Vis spectroscopy (Fig. S11). In all cases, the coatings exhibited transmittance values above 90% across the entire spectral region above 400 nm.

The gel fraction of the coatings was evaluated after extracting the soluble fraction in acetone for 24 h, and the results are summarized in Table 3. For the coatings cured by LED light, despite the considerable difference in the acrylate conversion value (Table 2), the insoluble fraction was quite similar in all the cases (higher than 90% for all three formulations), indicating the formation of well-developed crosslinked networks. On the other hand, the DS-IPDA coating, cured under the mercury-xenon lamp, showed a considerably lower value of gel fraction compared to its LED-cured counterpart (DS-IPDA 100), although both systems reached a similar double bond conversion of around 65 % after 120 s irradiation. This discrepancy suggests differences in network architecture: a plausible explanation is that the thiyl radicals formed by cleavage of the disulfide bond may react with the double bond both forming short chains and eventually giving intramolecular addition, producing cyclic products and reducing the effective crosslink density [65].

The thermal properties of photocured DS-IPDA/PEGDA coatings were investigated by performing DSC measurements. The values of the glass transition temperatures (T_g) for all the coatings tested are listed in Table 3, while DSC curves are represented in Fig. S7. For LED-cured coatings, the addition of PEGDA to DS-IPDA led to a decrease in the T_g: the value was 81 °C for DS-IPDA 100 and diminished to 37 °C in the presence of 50% w/w of PEGDA. These results confirm the hypothesis that earlier vitrification onset reduces the double bond conversion with increasing DS-IPDA content. In line with the value of T_g measured, DS-IPDA 100 coatings were found to be brittle, whilst those from DS-IPDA/PEGDA demonstrated a higher degree of flexibility. As seen for the gel fraction, also the T_g of the self-initiated DS-IPDA coating was lower than that of the DS-IPDA 100 counterpart, being 45 °C, further supporting the formation of a network with a distinct architecture under broadband irradiation.

The wettability of DS-IPDA/PEDGA photocured coatings was assessed through contact angle analysis. Both polar (water) and apolar (hexadecane) solvents were employed for the evaluation of the surface wettability. The contact angle values acquired using the two solvents, and the surface energies of the three different coatings with the respective polar and dispersive components are reported in Table 3. The contact angles of water and hexadecane were found to be analogous to those reported in the existing literature concerning other photocured coatings polymerized using disulfide-containing acrylate monomers [56,66,67]. However, when the PEGDA amount was increased in the LED cured formulations, a decrease in the water contact angle value was noted, reasonably due to the higher hydrophilicity of the comonomer. A similar trend was highlighted for the contact angle values measured with hexadecane, which showed an increase in the lipophilicity of DS-IPDA/PEDGA coating with increasing PEGDA amount. The DS-IPDA coating had a somewhat lower water contact angle that DS-IPDA 100. This may be attributed to the effect of UV-C irradiation, which may increase the hydrophilicity of polymers [68]. Given the contact angle values, the surface energy of coatings was computed using the Owens-Wendt geometric mean method [60]. As reported in Table 3, different values of surface energies were obtained, with a slight increase in the γ_S, and thus γ_S^P and γ_S^D components, with the increase of PEGDA amount in the formulation, reaching the maximum value for the DS-IPDA 50 sample.

The hardness of the coatings was assessed through a shore D durometer for the various formulations prepared in the form of films. DS-IPDA 100 and DS-IPDA 75 coatings displayed the highest hardness, while for DS-IPDA 50, having a higher concentration of PEGDA, the hardness was slightly lower (Table 3). It was not possible to evaluate the hardness of DS-IPDA and PEGDA films since both broke during the measurement.

The adhesion on glass substrate was evaluated through the X-cut method. DS-IPDA and DS-IPDA 100 were characterized by a good adhesion to glass: the coatings were detached just in small areas along the cuts, thus following the method's scale they have a score of 2 out of 5. Instead, both DS-IPDA 75 and DS-IPDA 50, as well as the reference PEGDA coating were completely detached from the substrate, scoring 5 out of 5. The urethane groups are able to form hydrogen bonds with the silanols on the glass surface, thus samples with a higher content of such groups may show better adhesion to glass.

The solvent resistance of the LED photocured coatings was assessed visually inspecting the film after rubbing them with a cotton pad soaked in ethyl acetate. Looking at the values reported in Table 3, as they have only a comparative significance, one can confirm that samples containing the most significant amount of PEGDA (DS-IPDA 50), assuring the highest value of double bond conversion (83%), have better chemical resistance to ethyl acetate.

3.4. Self-healing

The quantitative and qualitative examination of the self-healing properties of DS-IPDA/PEGDA coatings was conducted by optical microscopy. Scratches performed employing a surgical blade or a sharp metal tip on the surface of the coatings were analysed before and after heat treatment to understand the extent of the healing process.

As previously assessed by our group for photocured disulfide-containing acrylate coatings [56], heat-induced self-healing of surface

Table 4
Temperature of the healing treatment T_h, ΔT, and healing efficiency calculated as the percent decrease of the width of the damaged area.

Formulation	T_h [°C]	$\Delta T = T_h - T_g$	Healing efficiency [%]
DS-IPDA	100	55	42 ± 3
DS-IPDA 100	130	59	42 ± 3
DS-IPDA 100	100	19	36 ± 4
DS-IPDA 75	85	20	68 ± 10
DS-IPDA 50	55	18	95 ± 5

scratches could be easily achieved by working at a temperature slightly higher than the T_g of the cured coatings. Therefore, DS-IPDA and DS-IPDA/PEGDA coatings were heat-treated in an oven at a temperature at least 20 °C above their glass transition temperatures. The difference between the healing temperature and the T_g is indicated as ΔT. Optical microscope images were taken before and after the heat treatment, using some defects present in the coatings for benchmarking purposes.

Surface scratches with widths ranging from 7 to 25 μm were made on the surface of coatings with a sharp metal tip. The coatings were healed in the oven without any applied pressure, and the reduction of the width of the damaged area was assessed. The optical microscope images are shown in Figs. S9–S13 and the results are summarized in Table 4. Overall, healing efficiency strongly depended on network composition and on the temperature difference between the healing temperature and T_g (ΔT). Healing can be ascribed both to urethane functionalities by hydrogen bonding and disulfide groups through exchange reactions, as reported in Ref. [57]. Comparing samples DS-IPDA and DS-IPDA 100 healed with similar ΔT one can notice that the decrease of the number of available disulfide groups due to the self-initiated curing did not affect the healing efficiency for surface scratches, thus indicating that a sufficient number of disulfides was still present in the network. Despite the lowering of the concentration of both urethane and disulfide groups with the addition of PEGDA, a marked increase of the healing efficiency appeared with increasing PEGDA concentrations, indicating that self-healing was enhanced by the mobility of the network. On the contrary, PEGDA coatings taken as reference did not show any self-healing ability (Fig. S14). For comparison, Zhang et al., who used the same urethane acrylate monomer combined with 40 to 80 % of a monoacrylate diluent and an acrylate modified silica nanofiller used as a crosslinker, reported nearly complete scratch healing after prolonged UV-assisted treatment above T_g (UV light for 12 h at 50 °C) [57]. In contrast, the present systems achieve comparable healing under purely thermal activation and shorter treatment times, highlighting the efficiency of the formulation and network design.

Healing of thin surface scratches obtained with a surgical blade was evaluated qualitatively. As demonstrated in Fig. 8, a 10 min treatment resulted in partial healing of the scratches on DS-IPDA 100, but was insufficient to fully restore the surface of the coating. Even after 30 min of treatment at 100 °C, complete healing of the surface scratches was not achieved. For thin scratches, when a higher ΔT was employed, the coating self-healing was more effective, as demonstrated by Fig. 8; this can be reasonably attributed to the enhanced chain movement and, consequently, to a higher extent of disulfide metathesis reaction. In the latter case, with a ΔT of 50 °C between the treatment temperature and the T_g of the coating, almost all surface scratches were recovered after 10 min of heating.

In the case of PEGDA-containing coatings (i.e., DS-IPDA 75 and DS-IPDA 50) healing was performed at a temperature about 20 °C higher than the T_g of each coating, at 85 °C and 55 °C for DS-IPDA 75 and DS-IPDA 50, respectively. Almost complete healing of surface scratches

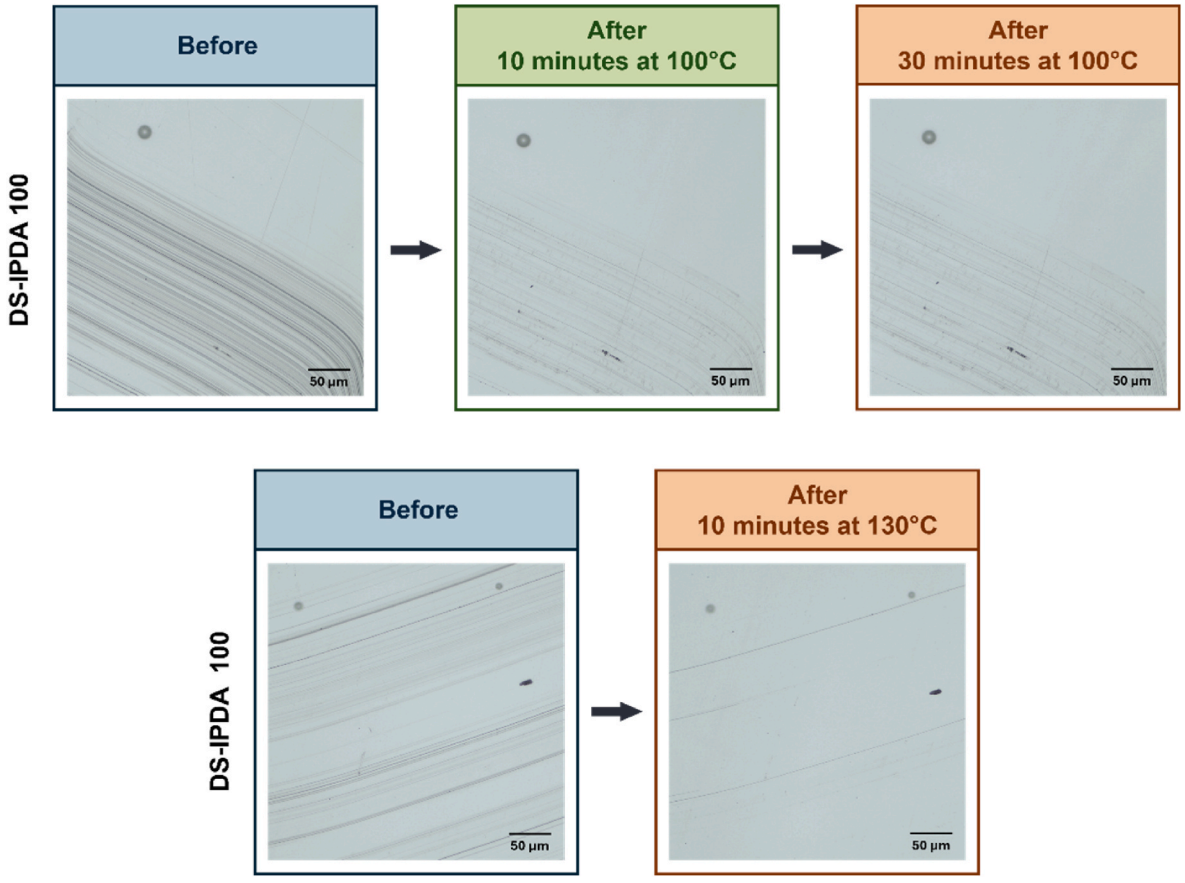

Fig. 8. Optical microscope images showing the healing of surface scratches on DS-IPDA 100 coating with a 100 °C heat treatment (top) and with a 130 °C heat treatment (bottom).

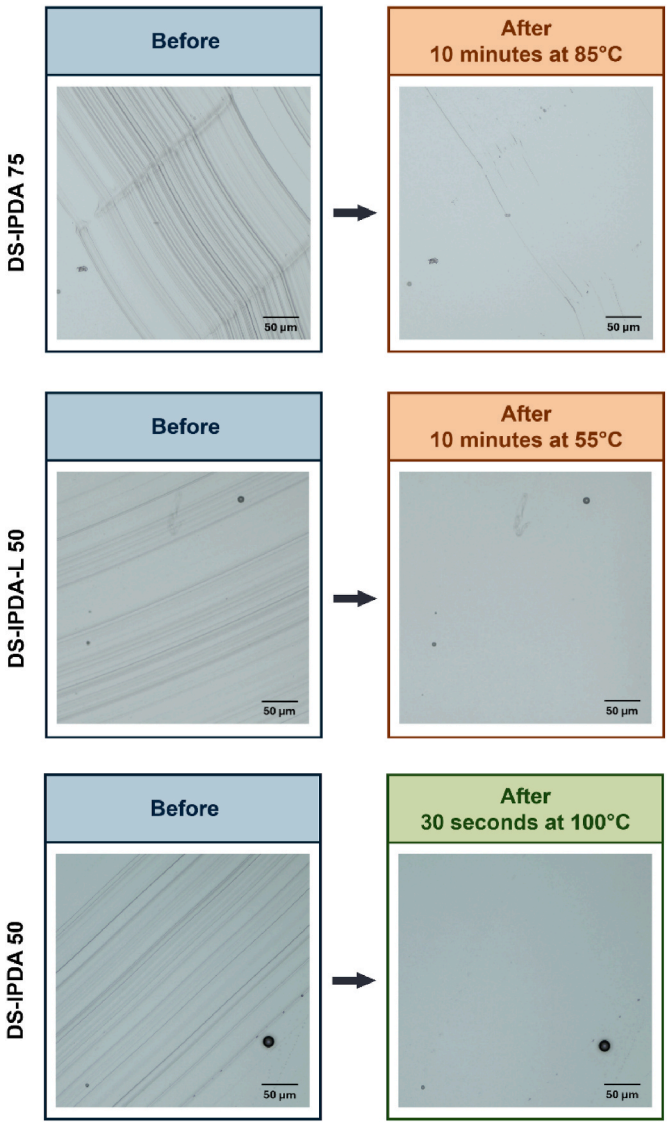

Fig. 9. Optical microscope images showing the healing of surface scratches on DS-IPDA 75 coatings with an 85 °C heat treatment, on DS-IPDA 50 coatings with a 55 °C heat treatment and DS-IPDA 50 coatings with a short heat treatment at 100 °C.

could be achieved after only 10 min of treatment, as reported in Fig. 9. Also in this case, both samples showed better healing compared to DS-IPDA 100 coatings, with the best results obtained for DS-IPDA 50 coatings. As depicted in Fig. 9, surface scratches present on coatings were fully recovered after 10 min of treatment at 55 °C.

Due to the outstanding healing ability of DS-IPDA 50, additional trials were conducted to determine if a more significant temperature difference between the T_g and the processing temperature could lead to a faster recovery process. When the coating was treated at 100 °C ($\Delta T \approx 65$ °C), surface scratches were healed after only 30 s of treatment in the oven (Fig. 9).

Finally, the ability to heal cuts was tested for the coatings displaying the best healing efficiencies for surface scratches, i.e, DS-IPDA 75 and DS-IPDA 50. Cuts with a width of about 5 – 10 µm were obtained with a surgical blade on 770 µm thick films, that were subsequently healed in a heated press under a force of 0.5 – 0.7 ton. In this case, we observed that for the DS-IPDA 75 coating (Fig. S15) the damaged area bordering the cut was fully healed, and the width of the cut itself decreased by 55 ± 4 % after healing for 15 min at 85 °C. For the DS-IPDA 50 coating little damage was noticeable beside the cut. After healing for 15 min at 55 °C the cut width decreased by 34 ± 6 % (Fig. S16). Thus, in this case, the material containing the highest amount of disulfide and urethane groups showed the best healing efficiency.

All these results underlined the complex interplay between network mobility, and thus glass transition temperature, and functional groups content in determining the healing ability. It can be deduced that while surface scratch recovery appears primarily governed by segmental mobility, effective repair of deeper cuts requires a sufficient density of dynamic functionalities to enable extensive bond exchange and network rearrangement.

4. Conclusions

In this study, a simple two-step procedure was employed to successfully synthesize an aliphatic long-chain polyurethane diacrylate monomer containing disulfide bonds (DS-IPDA). Photocuring analyses showed how DS-IPDA underwent a cleavage reaction when exposed to the broadband UV radiation of a mercury-xenon lamp, including UV-C light, resulting in the breakdown of disulfide bonds and the production of reactive thiyl radicals able to start the polymerization reaction (i.e., self-initiation), obtaining a 90% conversion of the acrylic double bonds. When the same monomer was exposed to longer wavelengths (around 365 nm) disulfide cleavage did not occur, ensuring a higher amount of available dynamic covalent bonds in the networks, but requiring the use of a photoinitiator. DS-IPDA was then mixed in different weight ratios with PEGDA to reduce its viscosity and decrease the final glass transition temperature of the photocured material. In this case, UV LED light with an emission around 365 nm was used for the photocuring reaction to maximize the amount of available sulfur-sulfur bond in the UV-cured coatings. High values of acrylic double bond conversion (83%) and gel fraction (96%) were reached for the DS-IPDA 50 material (containing 50 wt% PEGDA), which exhibited the lowest glass transition temperature value once cured ($T_g \approx 37$ °C). The potential of DS-IPDA based coatings, both self-initiated or cured in the presence of photoinitiator with the 365 nm LED source, to undergo self-repair was evaluated. It was demonstrated that, under mild conditions, the coatings could heal surface scratches after a short thermal treatment at temperatures approximately 20 to 60 °C above the T_g of the photocured networks. The healing time depended on the temperature difference (ΔT) between the T_g and the healing temperature: larger ΔT values resulted in shorter healing times. The LED-cured DS-IPDA/PEGDA coatings were also capable of partially healing cuts when heated under applied pressure. The results indicate that damage healing, particularly for defects with different morphologies, is governed by a complex interplay between network mobility and functional group content.

In conclusion, the findings presented offer novel insights and perspectives for the development of photoinitiator-free as well as dynamic and responsive UV-curable coatings based on a disulfide-containing polyurethane acrylate monomer. Interestingly, these features may enhance sustainability by reducing the use of chemical additives in the formulation, eliminating the need for potentially migrating photoinitiators, and imparting healability to the photocured coatings.

CRediT authorship contribution statement

Alberto Spessa: Writing – original draft, Visualization, Methodology, Investigation, Conceptualization. **Franca Castiglione:** Writing – original draft, Visualization, Methodology, Investigation. **Alice Rosanna Maggioni:** Writing – original draft, Methodology, Investigation. **Roberta Bongiovanni:** Writing – review & editing, Supervision, Resources, Methodology, Conceptualization. **Sara Dalle Vacche:** Writing – review & editing, Writing – original draft, Visualization, Supervision, Methodology, Investigation, Conceptualization. **Alessandra Vitale:** Writing – review & editing, Supervision, Resources, Methodology, Conceptualization.

Funding

This work was supported by the Italian Ministry of University and Research (MUR) [DM 1061/2021 PON-Dottorati di ricerca su tematiche green e dell'innovazione]

Declaration of competing interest

The authors declare that they have no known competing financial interests or personal relationships that could have appeared to influence the work reported in this paper.

Appendix A. Supplementary data

Supplementary data to this article can be found online at https://doi.org/10.1016/j.polymer.2026.130200.

Data availability

Data will be made available on request.

References

[1] A. Vitale, S. Molina-Gutiérrez, W.S.J. Li, S. Caillol, V. Ladmiral, P. Lacroix-Desmazes, S. Dalle Vacche, Biobased composites by photoinduced polymerization of cardanol methacrylate with microfibrillated cellulose, Materials 15 (2022) 339, https://doi.org/10.3390/ma15010339.

[2] S. Molina-Gutiérrez, S. Dalle Vacche, A. Vitale, V. Ladmiral, S. Caillol, R. Bongiovanni, P. Lacroix-Desmazes, Photoinduced polymerization of eugenol-derived methacrylates, Molecules 25 (2020) 3444, https://doi.org/10.3390/molecules25153444.

[3] Y. Yagci, S. Jockusch, N.J. Turro, Photoinitiated polymerization: advances, challenges, and opportunities, Macromolecules 43 (2010) 6245–6260, https://doi.org/10.1021/ma1007545.

[4] E. Rossegger, Y. Li, H. Frommwald, S. Schlögl, Vat photopolymerization 3D printing with light-responsive thiol-norbornene photopolymers, Monatsh. Chem. 154 (2023) 473–480, https://doi.org/10.1007/s00706-022-03016-5.

[5] J.V. Crivello, E. Reichmanis, Photopolymer materials and processes for advanced technologies, Chem. Mater. 26 (2014) 533–548, https://doi.org/10.1021/cm402262g.

[6] M. Topa-Skwarczyńska, M. Jankowska, A. Gruchała-Hałat, F. Petko, M. Galek, J. Ortyl, High-performance photoinitiating systems for new generation dental fillings, Dent. Mater. 39 (2023) 729–742, https://doi.org/10.1016/j.dental.2023.06.003.

[7] J. Tang, X. Xu, X. Shen, C. Kuang, H. Chen, M. Shi, N. Huang, Ketocoumarin-based photoinitiators for high-sensitivity two-photon lithography, ACS Appl. Polym. Mater. 5 (2023) 2956–2963, https://doi.org/10.1021/acsapm.3c00141.

[8] E.M. Maines, M.K. Porwal, C.J. Ellison, T.M. Reineke, Sustainable advances in SLA/DLP 3D printing materials and processes, Green Chem. 23 (2021) 6863–6897, https://doi.org/10.1039/D1GC01489G.

[9] J.P. Fouassier, J. Lalevée, Photoinitiators Structures, Reactivity and Applications in Polymerization, Wiley-VCH Verlag GmbH & Co. KGaA, Weinheim, Germany, 2021.

[10] R. Bongiovanni, S.D. Vacche, A. Vitale, Photoinduced processes as a way to sustainable polymers and innovation in polymeric materials, Polymers 13 (2021) 2293, https://doi.org/10.3390/polym13142293.

[11] U. Shaukat, E. Rossegger, S. Schlögl, Thiol–acrylate based vitrimers: from their structure–property relationship to the additive manufacturing of self-healable soft active devices, Polymer 231 (2021) 124110, https://doi.org/10.1016/j.polymer.2021.124110.

[12] A. Spessa, F. Castiglione, A. Vitale, R. Bongiovanni, S. Dalle Vacche, Fats and oils as a sustainable source of photopolymerizable monomers, Polymers 16 (2024) 3570, https://doi.org/10.3390/polym16243570.

[13] T. Scherzer, VUV-induced photopolymerization of acrylates, Macromol. Chem. Phys. 213 (2012) 324–334, https://doi.org/10.1002/macp.201100485.

[14] M. Biedermann, J.-E. Ingenhoff, M. Zurfluh, L. Richter, T. Simat, A. Harling, W. Altkofer, R. Helling, K. Grob, Migration of mineral oil, photoinitiators and plasticisers from recycled paperboard into dry foods: a study under controlled conditions, Food Addit. Contam. 30 (2013) 885–898, https://doi.org/10.1080/19440049.2013.786189.

[15] X. Ji, J. Liang, J. Liu, J. Shen, Y. Li, Y. Wang, C. Jing, S.A. Mabury, R. Liu, Occurrence, fate, human exposure, and toxicity of commercial photoinitiators, Environ. Sci. Technol. 57 (2023) 11704–11717, https://doi.org/10.1021/acs.est.3c02857.

[16] C.P. Vázquez, C. Joly-Duhamel, B. Boutevin, Photopolymerization without photoinitiator of bismaleimide-containing oligo(oxypropylene)s: effect of oligoethers chain length, Macromol. Chem. Phys. 210 (2009) 269–278, https://doi.org/10.1002/macp.200800510.

[17] Q. Wang, G. Chen, Y. Cui, J. Tian, M. He, J.-W. Yang, Castor oil based biothiol as a highly stable and self-initiated oligomer for photoinitiator-free UV coatings, ACS Sustainable Chem. Eng. 5 (2017) 376–381, https://doi.org/10.1021/acssuschemeng.6b01756.

[18] A. Jagtap, A. More, A review on self-initiated and photoinitiator-free system for photopolymerization, Polym. Bull. 79 (2022) 8057–8091, https://doi.org/10.1007/s00289-021-03887-4.

[19] O. Daikos, S. Naumov, W. Knolle, K. Heymann, T. Scherzer, Peculiarities of the photoinitiator-free photopolymerization of pentabrominated and pentafluorinated aromatic acrylates and methacrylates, Phys. Chem. Chem. Phys. 18 (2016) 32369–32377, https://doi.org/10.1039/C6CP06549J.

[20] R. Bongiovanni, M. Sangermano, G. Malucelli, A. Priola, UV curing of photoinitiator-free systems containing bismaleimides and diacrylate resins: bulk and surface properties, Prog. Org. Coating 53 (2005) 46–49, https://doi.org/10.1016/j.porgcoat.2004.11.009.

[21] N.B. Cramer, J.P. Scott, C.N. Bowman, Photopolymerizations of thiol−Ene polymers without photoinitiators, Macromolecules 35 (2002) 5361–5365, https://doi.org/10.1021/ma0200672.

[22] M. Zhang, S. Jiang, Y. Gao, J. Nie, F. Sun, Design of a disulfide bond-containing photoresist with extremely low volume shrinkage and excellent degradation ability for UV-nanoimprinting lithography, Chem. Eng. J. 390 (2020) 124625, https://doi.org/10.1016/j.cej.2020.124625.

[23] A. Chemtob, N. Feillée, C. Vaulot, C. Ley, D. Le Nouen, Self-photopolymerization of poly(disulfide) oligomers, ACS Omega 4 (2019) 5722–5730, https://doi.org/10.1021/acsomega.9b00021.

[24] J. Chen, S. Jiang, Y. Gao, F. Sun, Reducing volumetric shrinkage of photopolymerizable materials using reversible disulfide-bond reactions, J. Mater. Sci. 53 (2018) 16169–16181, https://doi.org/10.1007/s10853-018-2778-2.

[25] M. Zhang, S. Jiang, Y. Gao, J. Nie, F. Sun, UV-Nanoimprinting lithography photoresists with no photoinitiator and low polymerization shrinkage, Ind. Eng. Chem. Res. 59 (2020) 7564–7574, https://doi.org/10.1021/acs.iecr.9b07103.

[26] C.W. Bookwalter, D.L. Zoller, P.L. Ross, M.V. Johnston, Bond-selective photodissociation of aliphatic disulfides, J. Am. Soc. Mass Spectrom. 6 (1995) 872–876, https://doi.org/10.1016/1044-0305(95)00483-T.

[27] H.M. Dizman, N. Arsu, Rapid and sensitive colorimetric determination of dopamine and serotonin in solution and polymer matrix with photochemically prepared and N-acetyl-L-cysteine functionalized gold nanoparticles, Mater. Today Commun. 35 (2023) 105599, https://doi.org/10.1016/j.mtcomm.2023.105599.

[28] E.M. Maines, M.A. Polley, G. Haugstad, B. Zhao, T.M. Reineke, C.J. Ellison, Mechanical recycling of 3D-Printed thermosets for reuse in vat photopolymerization, ACS Appl. Polym. Mater. 6 (2024) 4625–4633, https://doi.org/10.1021/acsapm.4c00184.

[29] X. Lopez De Pariza, O. Varela, S.O. Catt, T.E. Long, E. Blasco, H. Sardon, Recyclable photoresins for light-mediated additive manufacturing towards loop 3D printing, Nat. Commun. 14 (2023), https://doi.org/10.1038/s41467-023-41267-w.

[30] V.S.D. Voet, J. Guit, K. Loos, Sustainable photopolymers in 3D printing: a review on biobased, biodegradable, and recyclable alternatives, Macromol. Rapid Commun. 42 (2021) 2000475, https://doi.org/10.1002/marc.202000475.

[31] S. Yang, K. Lian, P. Tian, D. Lu, J. Zhang, Photocurable vitrimers with malleable and self-healing trade-off enabled by manipulating dynamic boronic ester bonds, Colloids Surf. A Physicochem. Eng. Asp. 702 (2024) 135103, https://doi.org/10.1016/j.colsurfa.2024.135103.

[32] J.M. Winne, L. Leibler, F.E. Du Prez, Dynamic covalent chemistry in polymer networks: a mechanistic perspective, Polym. Chem. 10 (2019) 6091–6108, https://doi.org/10.1039/C9PY01260E.

[33] B. Zhang, K. Kowsari, A. Serjouei, M.L. Dunn, Q. Ge, Reprocessable thermosets for sustainable three-dimensional printing, Nat. Commun. 9 (2018), https://doi.org/10.1038/s41467-018-04292-8.

[34] E. Rossegger, R. Höller, D. Reisinger, M. Fleisch, J. Strasser, V. Wieser, T. Griesser, S. Schlögl, High resolution additive manufacturing with acrylate based vitrimers using organic phosphates as transesterification catalyst, Polymer 221 (2021) 123631, https://doi.org/10.1016/j.polymer.2021.123631.

[35] S. Engelen, B. Daelman, J.M. Winne, F.E. Du Prez, Activated phenyl ester vitrimers, Macromol, Rapid Commun 46 (2025), https://doi.org/10.1002/marc.202400790.

[36] F. Zhang, P. Ju, M. Pan, D. Zhang, Y. Huang, G. Li, X. Li, Self-healing mechanisms in smart protective coatings: a review, Corros. Sci. 144 (2018) 74–88, https://doi.org/10.1016/j.corsci.2018.08.005.

[37] Z. Guo, Research advances in UV-curable self-healing coatings, RSC Adv. 12 (2022) 32429–32439, https://doi.org/10.1039/D2RA06089B.

[38] S. Zhou, N. Qi, Z. Zhang, P. Jiang, A. Li, Y. Lu, X. Su, Recent progress in intrinsic self-healing polymer materials: mechanisms, challenges and potential applications in oil and gas development, Chem. Eng. J. 511 (2025) 161906, https://doi.org/10.1016/j.cej.2025.161906.

[39] T. Li, Z.P. Zhang, M.Z. Rong, M.Q. Zhang, Self-healable and thiol–ene UV-curable waterborne polyurethane for anticorrosion coating, J. Appl. Polym. Sci. 136 (2019) 47700, https://doi.org/10.1002/app.47700.

[40] D. Zhao, S. Liu, Y. Wu, T. Guan, N. Sun, B. Ren, Self-healing UV light-curable resins containing disulfide group: synthesis and application in UV coatings, Prog. Org. Coating 133 (2019) 289–298, https://doi.org/10.1016/j.porgcoat.2019.04.060.

[41] L.M. Sáiz, M.G. Prolongo, V. Bonache, A. Jiménez-Suárez, S.G. Prolongo, Self-healing materials based on disulfide bond-containing acrylate networks, Polym. Test. 117 (2023) 107832, https://doi.org/10.1016/j.polymertesting.2022.107832.

[42] J.M. Matxain, J.M. Asua, F. Ruipérez, Design of new disulfide-based organic compounds for the improvement of self-healing materials, Phys. Chem. Chem. Phys. 18 (2016) 1758–1770, https://doi.org/10.1039/C5CP06660C.

[43] H. Mutlu, E.B. Ceper, X. Li, J. Yang, W. Dong, M.M. Ozmen, P. Theato, Sulfur chemistry in polymer and materials science, Macromol. Rapid Commun. 40 (2019) 1800650, https://doi.org/10.1002/marc.201800650.

[44] M. Pepels, I. Filot, B. Klumperman, H. Goossens, Self-healing systems based on disulfide–thiol exchange reactions, Polym. Chem. 4 (2013) 4955, https://doi.org/10.1039/c3py00087g.
[45] M. Wang, H. Gao, Z. Wang, Y. Mao, J. Yang, B. Wu, L. Jin, C. Zhang, Y. Xia, K. Zhang, Rapid self-healed vitrimers via tailored hydroxyl esters and disulfide bonds, Polymer 248 (2022) 124801, https://doi.org/10.1016/j.polymer.2022.124801.
[46] Y. Deng, Q. Zhang, D. Qu, H. Tian, B.L. Feringa, A chemically recyclable crosslinked polymer network enabled by orthogonal dynamic covalent chemistry, Angew. Chem. Int. Ed. 61 (2022), https://doi.org/10.1002/anie.202209100.
[47] D. Zhao, Z. Du, S. Liu, Y. Wu, T. Guan, Q. Sun, N. Sun, B. Ren, UV light curable self-healing superamphiphobic coatings by photopromoted disulfide exchange reaction, ACS Appl. Polym. Mater. 1 (2019) 2951–2960, https://doi.org/10.1021/acsapm.9b00656.
[48] J. Huang, J. Zhang, G. Zhu, X. Yu, Y. Hu, Q. Shang, J. Chen, L. Hu, Y. Zhou, C. Liu, Self-healing, high-performance, and high-biobased-content UV-curable coatings derived from rubber seed oil and itaconic acid, Prog. Org. Coating 159 (2021) 106391, https://doi.org/10.1016/j.porgcoat.2021.106391.
[49] B. Wang, Z. Li, X. Liu, L. Li, J. Yu, S. Li, G. Guo, D. Gao, Y. Dai, Preparation of epoxy resin with disulfide-containing curing agent and its application in self-healing coating, Materials 16 (2023) 4440, https://doi.org/10.3390/ma16124440.
[50] S. Jin, H. Jeon, S.-M. Kim, M. Lee, C. Park, Y. Joo, J. Seo, D.X. Oh, J. Park, Self-healable spray paint coatings based on polyurethanes with thermal stability: effects of disulfides and diisocyanates, Prog. Org. Coating 198 (2025) 108931, https://doi.org/10.1016/j.porgcoat.2024.108931.
[51] M. Liu, J. Zhong, Z. Li, J. Rong, K. Yang, J. Zhou, L. Shen, F. Gao, X. Huang, H. He, A high stiffness and self-healable polyurethane based on disulfide bonds and hydrogen bonding, Eur. Polym. J. 124 (2020) 109475, https://doi.org/10.1016/j.eurpolymj.2020.109475.
[52] S. Nevejans, N. Ballard, M. Fernández, B. Reck, J.M. Asua, Flexible aromatic disulfide monomers for high-performance self-healable linear and cross-linked poly (urethane-urea) coatings, Polymer 166 (2019) 229–238, https://doi.org/10.1016/j.polymer.2019.02.001.
[53] X. Li, R. Yu, Y. He, Y. Zhang, X. Yang, X. Zhao, W. Huang, Self-healing polyurethane elastomers based on a disulfide bond by digital light processing 3D printing, ACS Macro Lett. 8 (2019) 1511–1516, https://doi.org/10.1021/acsmacrolett.9b00766.
[54] H. Zhou, C. Liu, J. Huang, Y. Li, G. Zhu, C. Lu, J. Yao, H. Xu, P. Zhao, High-performance, high biobased content, self-repairable, and recyclable biobased photopolymers for UV-curing 3D printing, Ind. Crop. Prod. 224 (2025) 120299, https://doi.org/10.1016/j.indcrop.2024.120299.
[55] K. Zheng, J. Wang, J. Chen, J. Hao, Z. Liu, S. Xing, J. Yang, D. Chen, High-strength and debondable UV-curable adhesive based on dual-dynamic network, Polym. Degrad. Stabil. 242 (2025) 111665, https://doi.org/10.1016/j.polymdegradstab.2025.111665.
[56] A. Spessa, R. Bongiovanni, A. Vitale, A novel disulfide-containing monomer for photoinitiator-free self-healable photocured coatings, Prog. Org. Coating 187 (2024) 108098, https://doi.org/10.1016/j.porgcoat.2023.108098.
[57] Y. Zhang, Y. Sheng, M. Wang, X. Lu, UV-curable self-healing, high hardness and transparent polyurethane acrylate coating based on dynamic bonds and modified nano-silica, Prog. Org. Coating 172 (2022) 107051, https://doi.org/10.1016/j.porgcoat.2022.107051.
[58] R. Bongiovanni, A. Medici, A. Zompatori, S. Garavaglia, C. Tonelli, Perfluoropolyether polymers by UV curing: design, synthesis and characterization, Polym. Int. 61 (2012) 65–73, https://doi.org/10.1002/pi.3149.
[59] Y. Liu, S. Li, L. Feng, H. Yu, X. Qi, W. Wei, J. Li, W. Dong, Novel disulfide-containing Poly(β-amino ester)-functionalised magnetic nanoparticles for efficient gene delivery, Aust. J. Chem. 69 (2016) 349, https://doi.org/10.1071/CH15293.
[60] D.K. Owens, R.C. Wendt, Estimation of the surface free energy of polymers, J. Appl. Polym. Sci. 13 (1969) 1741–1747, https://doi.org/10.1002/app.1969.070130815.
[61] ASTM Committee D01, Practice for Measuring MEK Resistance of Ethyl Silicate (Inorganic) Zinc-Rich Primers by Solvent Rub, 2020, https://doi.org/10.1520/D4752-20.
[62] S.H.M. Söntjens, R.A.E. Renken, G.M.L. van Gemert, T.A.P. Engels, A.W. Bosman, H.M. Janssen, L.E. Govaert, F.P.T. Baaijens, Thermoplastic elastomers based on strong and well-defined hydrogen-bonding interactions, Macromolecules 41 (2008) 5703–5708, https://doi.org/10.1021/ma800744c.
[63] T. Bultmann, N.P. Ernsting, Competition between geminate recombination and solvation of polar radicals following ultrafast photodissociation of bis(p-aminophenyl) disulfide, J. Phys. Chem. 100 (1996) 19417–19424, https://doi.org/10.1021/jp962151n.
[64] L. Milanesi, G.D. Reid, G.S. Beddard, C.A. Hunter, J.P. Waltho, Synthesis and photochemistry of a new class of photocleavable protein cross-linking reagents, Chem. Eur J. 10 (2004) 1705–1710, https://doi.org/10.1002/chem.200305405.
[65] D.M. Lynch, E.M. Scanlan, Thiyl radicals: versatile reactive intermediates for cyclization of unsaturated substrates, Molecules 25 (2020), https://doi.org/10.3390/molecules25133094.
[66] J. Xu, X. Rong, T. Chi, M. Wang, Y. Wang, D. Yang, F. Qiu, Preparation, characterization of UV-Curable waterborne polyurethane-acrylate and the application in metal iron surface protection, J. Appl. Polym. Sci. 130 (2013) 3142–3152, https://doi.org/10.1002/app.39539.
[67] J. Zhou, H. Xu, L. Tang, Facile fabrication of high performance hydrophilic anti-icing polyurethane methacrylate coatings cured via UV irradiation, Prog. Org. Coating 182 (2023) 107657, https://doi.org/10.1016/j.porgcoat.2023.107657.
[68] W. Simon, D. Klassen, M. Mottoul, S. Ponton, D. Brassard, J.-M. Raquez, A. Karthikeyan, M.-J. Dumont, J.R. Tavares, Long-lasting hydrophilicity induced by ultraviolet light on surface modified hydrophobic polylactic acid, J. Appl. Polym. Sci. 142 (2025) e57009, https://doi.org/10.1002/app.57009.